1 The Fundamental Classic Analysis of Edelbaum, Sackett and Malchow, with Additional Detailed Derivations and Extensions

1.1 Introduction

Important advances in the development of realistic simulation tools for the analysis of optimal transfers between general elliptic orbits using low-thrust electric ion engines were made in the early 1970s by a team of inspired scientists at the Massachusetts Institute of Technology (MIT) Draper Laboratory. This analysis and the resulting computer software are exposed in this chapter, and built on in the succeeding chapters, in particular for the creation of more accurate tools taking full advantage of the increasing speed of modern computers. Edelbaum [1] and his collaborators have used the method of averaging in order to eliminate the quickly varying orbit element for the spacecraft position along its orbit, leaving only the slowly varying elements that describe the instantaneous shape and orientation of the orbit during the transfer of the spacecraft. This is made possible due to the low acceleration imparted by the electric engines. The averaged rates are calculated by numerical quadrature, representing thereby the dynamical system quite accurately for numerical integration. A set of nonsingular orbit elements called the equinoctial elements are adopted in order to avoid any singularities for zero eccentricity and zero inclination during the numerical integrations. These singularities are unavoidable if the classical orbit elements are used instead.

Optimal control methodology is applied to develop the adjoint differential equations associated with each element for simultaneous integration with the dynamic equations, and the transfer trajectory is optimized by orienting the thrust acceleration vector in the optimal direction at each moment in time, leading to the creation of minimum-time trajectories. The indirect shooting method is used to converge on the guessed initial values of the adjoint or Lagrange multipliers in order to generate those initial values that meet the desired final conditions, solving thereby the two-point boundary value problem.

The important perturbations due to the earth's oblateness which precess the orbit, and the power degradation resulting from the damage incurred by the solar panels during the transit through the Van Allen belts, which in effect reduces the thrust magnitude of the thrusters, are also carried out by the three pioneers mentioned above. The averaging technique is thus employed for these perturbations because they too change or affect the trajectory, slowly, as was the case for the five slowly varying orbit elements.

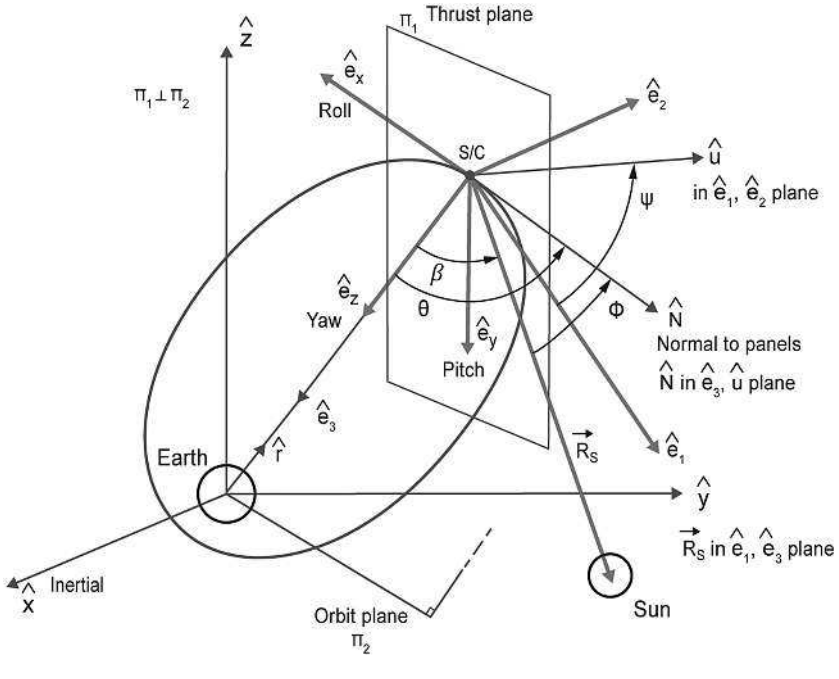

Figure 1.1 General configuration of spacecraft axes.

Spacecraft attitude constraints are also included to accommodate certain spacecraft configurations, such as for the case of the ion thrusters mounted on the negative roll face of the spacecraft and directed parallel to the roll axis. The solar panels are assumed to be flat and capable of rotation about their longitudinal axis. A proper combination of spacecraft roll and panels axis rotation can align the panels to fully face the Sun vector for maximum power output. The nominal attitude of the principle body-centered axes of the spacecraft shown in Figure 1.1 is such that these axes are aligned with a coordinate system made of the roll axis, the yaw axis and the pitch axis, with the roll axis in the orbit plane and orthogonal to the spacecraft–Earth radius vector, the yaw axis along the radius vector and the pitch axis normal to the orbit plane, with each positive direction specified in more detail in what follows.

Three attitude-constrained cases are investigated, namely, the zero roll and pitch case, free roll and zero pitch case, and the free roll, yaw and pitch case, also called the unconstrained case. The constrained case of zero roll is such that the panels cannot be oriented normal to the Sun vector, but must instead adopt the best orientation possible for maximum power extraction under the circumstances. Finally, in their analysis, Edelbaum et al. [1] assume that thrust is proportional to power with constant specific impulse I_{sp}, and efficiency.

The following sections describe many of these elements in some detail, with some new additional analysis for the zero roll case, which is important in its own right for trade studies.

The next chapters introduce the use of different orbit elements by also accounting for the fast variable for more accurate precision integration simulations, the use of the

Euler–Hill rotating frame for the resolution of the thrust acceleration vector components, and the use of gravitational perturbations due to the Sun and the Moon, among other additions and refinements.

Figures 1.1 through 1.6 are enhanced versions of the ones found in [1–3].

1.2 The Technique of Averaging

The variational equations for the classical elements in the Gaussian form with the components of the disturbing acceleration in the radial, transverse and out-of-plane directions are given by $\dot{a} = \frac{2a^2}{j}\left(es_{\theta^*}f_r + \frac{b}{r}f_\theta\right)$, $\dot{e} = \frac{1}{j}[bs_{\theta^*}f_r + \{(b+r)c_{\theta^*} + re\}f_\theta]$, $\dot{i} = \frac{rc_\theta}{j}f_h$, $\dot{\Omega} = \frac{rs_\theta}{js_i}f_h$, $\dot{\omega} = \frac{1}{je}[-bc_{\theta^*}f_r + (b+r)s_{\theta^*}f_\theta] - \frac{rs_\theta c_i}{js_i}f_h$, $\dot{M} = n + \frac{(1-e^2)^{1/2}}{je} \times [(bc_{\theta^*} - 2re)f_r - (b+r)s_{\theta^*}f_\theta]$ where a, e, i, Ω, ω and M are the classical orbit elements; $b = a(1-e^2)$ is the orbit parameter, $j = [\mu a(1-e^2)]^{1/2}$ is the orbit angular momentum, r is the radial distance defined by $r = b/(1+ec_{\theta^*})$, θ is the angular position defined by $\theta = \omega + \theta^*$, with θ^* the true anomaly, and f_r, f_θ and f_h are the components of the disturbing acceleration vector resolved along the rotating Euler–Hill coordinate axes.

These differential equations are singular for $e = 0$, and $i = 0$, and are therefore not suitable for integration when the running orbit is at, or very near the circular and/or the equatorial conditions. For example, the important application of transferring a spacecraft from a circular low orbit to a geostationary orbit requires the adoption of a set of equations that are nonsingular for these two conditions for proper integration. This book develops several such nonsingular sets for use by mission analysts and designers, allowing the development of flight guidance software to optimally carry out such important transfers. Chapter 8 shows how the singular equations depicted above are converted into the nonsingular form using a particular set of equinoctial elements. Analysts and software developers can be better equipped by using several different sets of the dynamic and multiplier theories from the simple thrust-only formulations, to more involved models such as with oblateness and luni-solar gravity perturbations, both in precision integration mode for exact simulations, and in averaged mode for approximate applications. This chapter begins by showing the averaging method used by Edelbaum et al. in the 1970s, with subsequent chapters developing more refined models for both academic and practical interests, and further research endeavors by specialists in space flight guidance.

The averaging technique is used to consider only the first approximation to the state and costate or adjoint differential equations for rapid numerical integration of these equations as opposed to the much slower precision integration of the unaveraged equations. The averaging technique of [4] effectively eliminates the short period variations in the state and costate variables and assumes that these variables vary slowly. This is the case in low-thrust transfer problems where the sixth orbital element, which varies rapidly as it describes the location of the spacecraft in its orbit, is effectively eliminated from the equations of interest, which concern then only the size, shape and orientation of the orbit, but not the actual location of the spacecraft along its orbit, as the first five state variables vary slowly over time.

The averaged Hamiltonian $\tilde{H}$ is then obtained from the unaveraged Hamiltonian H by way of

$$\tilde{H} = \frac{1}{T}\int_{t-\frac{T}{2}}^{t+\frac{T}{2}} H dt \tag{1.1}$$

where t stands for the current time and T for the current orbital period. The state and adjoint variables are held constant during the integration, which is carried out by numerical quadrature, such that the spacecraft is considered to ride a Keplerian orbit during the averaging integration procedure. Thus, the first approximations to the state and adjoint variables are obtained from the integration of the coupled Euler–Hill differential equations

$$\dot{\tilde{\mathbf{x}}}^T = \frac{\partial \tilde{H}}{\partial \tilde{\boldsymbol{\lambda}}} \tag{1.2}$$

$$\dot{\tilde{\boldsymbol{\lambda}}}^T = -\frac{\partial \tilde{H}}{\partial \tilde{\mathbf{x}}} \tag{1.3}$$

with $\tilde{\mathbf{x}}$ and $\tilde{\boldsymbol{\lambda}}$ standing for the averaged generic state and corresponding adjoint variables. These equations can then be integrated numerically with large time steps spanning several orbital periods.

1.3 Summary of the Mechanics of the Equinoctial Orbit Elements

A summary of the various calculations of the position and velocity vector components along the slowly rotating $\hat{\mathbf{f}}$, $\hat{\mathbf{g}}$, $\hat{\mathbf{w}}$ coordinate system shown in Figure 1.2 is shown next and can be found in [1, 2, 5]. The details of their derivations are shown in [5] and also in Chapter 2.

Considering only the first five elements a, h, k, p and q, the relations between these elements and the classical elements are given by

$$\begin{aligned} a &= a \\ h &= e\sin(\omega+\Omega) \\ k &= e\cos(\omega+\Omega) \\ p &= \tan\left(\frac{i}{2}\right)\sin\Omega \\ q &= \tan\left(\frac{i}{2}\right)\cos\Omega \end{aligned} \tag{1.4}$$

and

$$\begin{aligned} a &= a \\ e &= \left(h^2+k^2\right)^{1/2} \\ i &= 2\tan^{-1}\left(p^2+q^2\right)^{1/2} \\ \Omega &= \tan^{-1}(p/q) \\ \omega &= \tan^{-1}(h/k) - \tan^{-1}(p/q) \end{aligned} \tag{1.5}$$

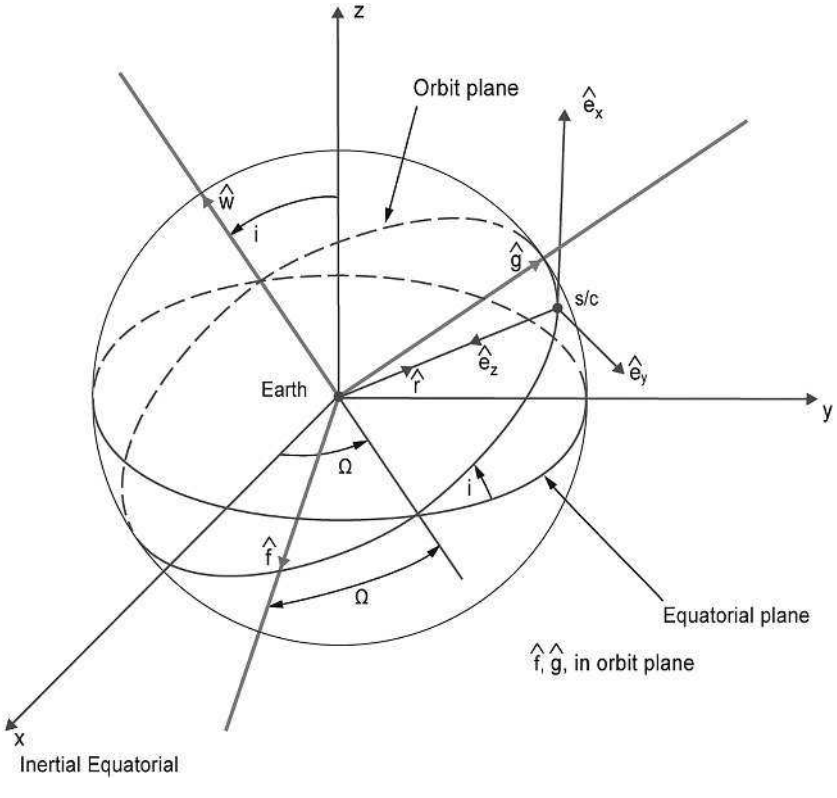

Figure 1.2 The Earth-centered equinoctial coordinate frame.

The fast variable or sixth element is selected as the eccentric longitude F which is related to the eccentric anomaly E by

$$F = E + \omega + \Omega \tag{1.6}$$

This element is eliminated from the dynamic equations by the averaging process. Figure 1.2 shows how the Earth-centered $\hat{\mathbf{f}}$, $\hat{\mathbf{g}}$, $\hat{\mathbf{w}}$ rotating frame is constructed by moving backwards by an angle Ω from the orbit ascending node for $\hat{\mathbf{f}}$, with $\hat{\mathbf{g}}$ in the orbital plane and 90 deg ahead, and with $\hat{\mathbf{w}}$ completing the triad. These unit vectors are given with respect to an inertial equatorial frame $\hat{\mathbf{x}}$, $\hat{\mathbf{y}}$, $\hat{\mathbf{z}}$ by

$$\begin{aligned}
\hat{\mathbf{f}} &= \frac{1}{(1+p^2+q^2)}\begin{bmatrix}(1-p^2+q^2)\\ 2pq\\ -2p\end{bmatrix} = \begin{pmatrix}f_1\\ f_2\\ f_3\end{pmatrix} = f_1\hat{\mathbf{x}} + f_2\hat{\mathbf{y}} + f_3\hat{\mathbf{z}}\\
\hat{\mathbf{g}} &= \frac{1}{(1+p^2+q^2)}\begin{bmatrix}2pq\\ (1+p^2-q^2)\\ 2q\end{bmatrix} = \begin{pmatrix}g_1\\ g_2\\ g_3\end{pmatrix} = g_1\hat{\mathbf{x}} + g_2\hat{\mathbf{y}} + g_3\hat{\mathbf{z}}\\
\hat{\mathbf{w}} &= \frac{1}{(1+p^2+q^2)}\begin{bmatrix}2p\\ -2q\\ (1-p^2+q^2)\end{bmatrix} = \begin{pmatrix}w_1\\ w_2\\ w_3\end{pmatrix} = w_1\hat{\mathbf{x}} + w_2\hat{\mathbf{y}} + w_3\hat{\mathbf{z}}
\end{aligned} \tag{1.7}$$

Given position and velocity vectors $\mathbf{r}$ and $\dot{\mathbf{r}}$, the equinoctial elements are calculated from

$$a = \left(\frac{2}{|\mathbf{r}|} - \frac{|\dot{\mathbf{r}}|^2}{\mu} \right)^{-1} \tag{1.8}$$

$$\mathbf{e} = -\frac{\mathbf{r}}{|\mathbf{r}|} - \frac{(\mathbf{r} \times \dot{\mathbf{r}}) \times \dot{\mathbf{r}}}{\mu} \tag{1.9}$$

$$\hat{\mathbf{w}} = \frac{\mathbf{r} \times \dot{\mathbf{r}}}{|\mathbf{r} \times \dot{\mathbf{r}}|} \tag{1.10}$$

$$p = \frac{w_1}{1 + w_3} \tag{1.11}$$

$$q = \frac{w_2}{1 + w_3} \tag{1.12}$$

μ being the Earth gravity constant, such that

$$h = \mathbf{e} \cdot \hat{\mathbf{g}} \tag{1.13}$$

$$k = \mathbf{e} \cdot \hat{\mathbf{f}} \tag{1.14}$$

The position coordinates X_1 and Y_1 are given in the $\hat{\mathbf{f}}$, $\hat{\mathbf{g}}$ frame by

$$X_1 = \mathbf{r} \cdot \hat{\mathbf{f}} \tag{1.15}$$

$$Y_1 = \mathbf{r} \cdot \hat{\mathbf{g}} \tag{1.16}$$

and the eccentric longitude F by

$$\cos F = k + \frac{\left(1 - k^2\beta\right) X_1 - hk\beta Y_1}{a\left(1 - h^2 - k^2\right)^{1/2}} \tag{1.17}$$

$$\sin F = h + \frac{\left(1 - h^2\beta\right) Y_1 - hk\beta X_1}{a\left(1 - h^2 - k^2\right)^{1/2}} \tag{1.18}$$

where

$$\beta = \frac{1}{1 + \left(1 - h^2 - k^2\right)^{1/2}} \tag{1.19}$$

From the definition of the mean longitude λ, in terms of the mean anomaly M namely,

$$\lambda = M + \omega + \Omega \tag{1.20}$$

the eccentric longitude can be extracted from Kepler's transcendental equation

$$\lambda = F - k \sin F + h \cos F \tag{1.21}$$

Thus,

$$\mathbf{r} = X_1\hat{\mathbf{f}} + Y_1\hat{\mathbf{g}} \tag{1.22}$$

$$\dot{\mathbf{r}} = \dot{X}_1\hat{\mathbf{f}} + \dot{Y}_1\hat{\mathbf{g}} \tag{1.23}$$

with

$$X_1 = a\left[\left(1 - h^2\beta\right)\cos F + hk\beta\sin F - k\right] \tag{1.24}$$

$$Y_1 = a\left[\left(1 - k^2\beta\right)\sin F + hk\beta\cos F - h\right] \tag{1.25}$$

$$\dot{X}_1 = \frac{na^2}{r}\left[hk\beta\cos F - \left(1 - h^2\beta\right)\sin F\right] \tag{1.26}$$

$$\dot{Y}_1 = \frac{na^2}{r}\left[\left(1 - k^2\beta\right)\cos F - hk\beta\sin F\right] \tag{1.27}$$

where the current mean motion n is given by

$$n = \left(\frac{\mu}{a^3}\right)^{1/2} \tag{1.28}$$

and the orbit equation

$$r = a\left(1 - kc_F - hs_F\right) \tag{1.29}$$

Letting $\boldsymbol{\lambda}$ and $\boldsymbol{\psi}$ represent the adjoint vectors in the equinoctial and classical representations, they are related by way of

$$\begin{pmatrix}\lambda_a\\ \lambda_h\\ \lambda_k\\ \lambda_p\\ \lambda_q\end{pmatrix} = \begin{pmatrix}1 & 0 & 0 & 0 & 0\\ 0 & \sin(\omega+\Omega) & 0 & 0 & \frac{\cos(\omega+\Omega)}{e}\\ 0 & \cos(\omega+\Omega) & 0 & 0 & \frac{-\sin(\omega+\Omega)}{e}\\ 0 & 0 & 2\sin\Omega\cos^2\frac{i}{2} & \frac{c_\Omega}{\tan\left(\frac{i}{2}\right)} & \frac{-c_\Omega}{\tan\left(\frac{i}{2}\right)}\\ 0 & 0 & 2\cos\Omega\cos^2\frac{i}{2} & \frac{-s_\Omega}{\tan\left(\frac{i}{2}\right)} & \frac{s_\Omega}{\tan\left(\frac{i}{2}\right)}\end{pmatrix}\begin{pmatrix}\psi_a\\ \psi_e\\ \psi_i\\ \psi_\Omega\\ \psi_\omega\end{pmatrix} \tag{1.30}$$

which can also be written in terms of the equinoctial elements

$$\begin{pmatrix}\lambda_a\\ \lambda_h\\ \lambda_k\\ \lambda_p\\ \lambda_q\end{pmatrix} = \begin{pmatrix}1 & 0 & 0 & 0 & 0\\ 0 & \frac{h}{(h^2+k^2)^{1/2}} & 0 & 0 & \frac{k}{(h^2+k^2)}\\ 0 & \frac{k}{(h^2+k^2)^{1/2}} & 0 & 0 & \frac{-h}{(h^2+k^2)}\\ 0 & 0 & \frac{2p}{(p^2+q^2)^{1/2}(1+p^2+q^2)} & \frac{q}{(p^2+q^2)} & \frac{-q}{(p^2+q^2)}\\ 0 & 0 & \frac{2q}{(p^2+q^2)^{1/2}(1+p^2+q^2)} & \frac{-p}{(p^2+q^2)} & \frac{p}{(p^2+q^2)}\end{pmatrix}\begin{pmatrix}\psi_a\\ \psi_e\\ \psi_i\\ \psi_\Omega\\ \psi_\omega\end{pmatrix} \tag{1.31}$$

The inverse relationships both in terms of the classical and equinoctial elements are obtained as

$$\begin{pmatrix}\psi_a\\ \psi_e\\ \psi_i\\ \psi_\Omega\\ \psi_\omega\end{pmatrix}=\begin{pmatrix}1 & 0 & 0 & 0 & 0\\ 0 & \sin(\omega+\Omega) & \cos(\omega+\Omega) & 0 & 0\\ 0 & 0 & 0 & \frac{1}{2}\sec^2\left(\frac{i}{2}\right)\sin\Omega & \frac{1}{2}\sec^2\left(\frac{i}{2}\right)\cos\Omega\\ 0 & e\cos(\omega+\Omega) & -e\sin(\omega+\Omega) & \tan\left(\frac{i}{2}\right)\cos\Omega & -\tan\left(\frac{i}{2}\right)\sin\Omega\\ 0 & e\cos(\omega+\Omega) & -e\sin(\omega+\Omega) & 0 & 0\end{pmatrix}\begin{pmatrix}\lambda_a\\ \lambda_h\\ \lambda_k\\ \lambda_p\\ \lambda_q\end{pmatrix} \tag{1.32}$$

$$\begin{pmatrix}\psi_a\\ \psi_e\\ \psi_i\\ \psi_\Omega\\ \psi_\omega\end{pmatrix}=\begin{pmatrix}1 & 0 & 0 & 0 & 0\\ 0 & \frac{h}{(h^2+k^2)^{1/2}} & \frac{k}{(h^2+k^2)^{1/2}} & 0 & 0\\ 0 & 0 & 0 & \frac{\frac{1}{2}p(1+p^2+q^2)}{(p^2+q^2)^{1/2}} & \frac{\frac{1}{2}q(1+p^2+q^2)}{(p^2+q^2)^{1/2}}\\ 0 & k & -h & q & -p\\ 0 & k & -h & 0 & 0\end{pmatrix}\begin{pmatrix}\lambda_a\\ \lambda_h\\ \lambda_k\\ \lambda_p\\ \lambda_q\end{pmatrix} \tag{1.33}$$

1.4 The Equations of Motion

The unaveraged differential equations for the equinoctial orbit elements and the variable spacecraft mass are derived in more detail in the next chapter. They have the following form:

$$\dot{\mathbf{z}}=\frac{2P}{mc}M(\mathbf{z},F)\,\hat{\mathbf{u}} \tag{1.34}$$

$$\dot{m}=\frac{-2P}{c^2} \tag{1.35}$$

with $\mathbf{z}$ standing for the five elements a, h, k, p and q, m for spacecraft mass and P for thruster beam power given by

$$P=\eta P_0 D(N)\frac{1}{R_s^2}\cos\phi \tag{1.36}$$

where P_0 is the maximum array power at 1 au, η the power efficiency factor, $D(N)$ the damage factor as a function of fluence N, with maximum value of 1, R_s the spacecraft–Sun distance in au, and ϕ the angle between the normal to the solar panels and the spacecraft–Sun vector. In the following and without any loss of generality, $\eta=1, R_s=1$ is assumed in [2] for the sake of the analysis such that

$$P=P_0\cos\phi \tag{1.37}$$

It is also assumed that the exhaust velocity c is constant,

$$c=I_{\text{sp}}g_0 \tag{1.38}$$

with constant specific impulse I_{sp}, and with g_0, the acceleration of gravity at the equator. The unit vector along the thrust direction is depicted by $\hat{\mathbf{u}}$, and the (5×3) matrix M is derived in Chapter 6 and given below as

$$M(\mathbf{z},F)=\frac{\partial\mathbf{z}}{\partial\dot{\mathbf{r}}} \tag{1.39}$$

where F was selected as the sixth independent orbital element in [2]. The seventh variable is the high-energy particle fluence $N(\mathbf{z})$ such that

$$\dot{N} = f(\mathbf{z}, F) \tag{1.40}$$

Letting H represent the unaveraged Hamiltonian and $\mathbf{x}$ the full seven-state vector, a first-order approximation to the state and costate is obtained by forming an averaged Hamiltonian $\tilde{H}$ from which the averaged canonical equations for the state and costate are derived:

$$\begin{aligned}\tilde{H}\left(\tilde{\mathbf{x}}, \tilde{\boldsymbol{\lambda}}, t\right) &= \frac{1}{T_0}\int_{t-\frac{T_0}{2}}^{t+\frac{T_0}{2}} H\left[\tilde{\mathbf{x}}, \tilde{\boldsymbol{\lambda}}, t, F(t), \hat{\mathbf{u}}(F(t))\right] dt \\ &= \frac{1}{T_0}\int_{-\pi}^{\pi} H\left[\tilde{\mathbf{x}}, \tilde{\boldsymbol{\lambda}}, t, F, \hat{\mathbf{u}}(F)\right]\frac{dt}{dF}dF = \int_{-\pi}^{\pi} HsdF\end{aligned} \tag{1.41}$$

From Kepler's equation, $\lambda = F - k\sin F + h\cos F = ndt$, we have

$$\begin{aligned}d\lambda &= dF - k\cos FdF - h\sin FdF \\ &= (1 - k\cos F - h\sin F)\, dF = ndt = \frac{2\pi}{T_0}dt\end{aligned} \tag{1.42}$$

where T_0 is the current Keplerian orbital period, $T_0 = \frac{2\pi}{n}$, such that

$$\frac{dt}{dF} = \frac{T_0}{2\pi}\left(1 - \tilde{k}\cos F - \tilde{h}\sin F\right) \tag{1.43}$$

The integrations are carried out with respect to F such that letting

$$s(\mathbf{z}, F) = \frac{1}{T_0}\frac{dt}{dF} = \frac{1}{2\pi}\frac{r}{a} \tag{1.44}$$

the canonical equations take the form

$$\dot{\tilde{\mathbf{x}}} = \left(\frac{\partial \tilde{H}}{\partial \tilde{\boldsymbol{\lambda}}}\right)^T = \int_{-\pi}^{\pi}\left(\frac{\partial H}{\partial \tilde{\boldsymbol{\lambda}}}\right)^T sdF \tag{1.45}$$

$$\dot{\tilde{\boldsymbol{\lambda}}} = -\left(\frac{\partial \tilde{H}}{\partial \tilde{\mathbf{x}}}\right)^T = -\int_{-\pi}^{\pi}\left[\left(\frac{\partial H}{\partial \tilde{\mathbf{x}}}\right)^T s + H\left(\frac{\partial s}{\partial \tilde{\mathbf{x}}}\right)^T\right] dF \tag{1.46}$$

the state and costate being held constant during the integrations. As noted in [2], the $\frac{\partial H}{\partial \tilde{\boldsymbol{\lambda}}}$ and $-\frac{\partial H}{\partial \tilde{x}}$ are the unaveraged state and costate equations, and the $\frac{\partial s}{\partial \tilde{\mathbf{x}}}$ partials are just

$$\frac{\partial s}{\partial \tilde{h}} = -\frac{1}{2\pi}\sin F \tag{1.47}$$

$$\frac{\partial s}{\partial \tilde{k}} = -\frac{1}{2\pi}\cos F \tag{1.48}$$

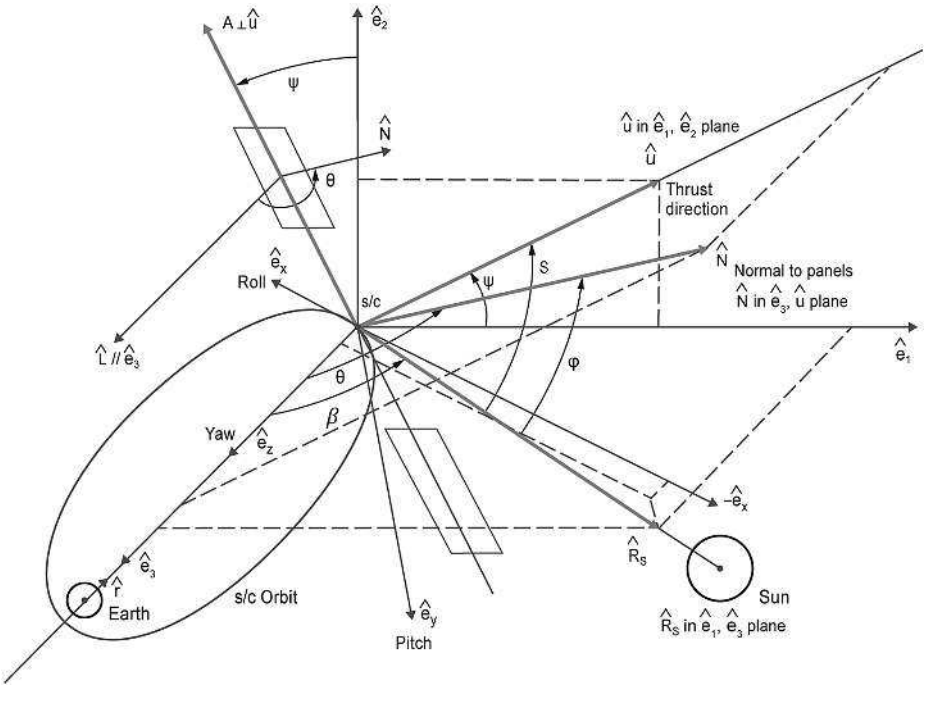

Figure 1.3 Thrust and solar panels' orientation angles.

1.5 The Averaged State and Costate Differential Equations for the Thrust-Constrained Case $\hat{\mathbf{u}} \perp \hat{\mathbf{r}}$

In [2], an important operational constraint is considered whereby the thrust vector is orthogonal to the spacecraft–Earth vector, such that $\hat{\mathbf{u}} \perp \hat{\mathbf{r}}$ at all times. It is then convenient to express $\hat{\mathbf{u}}$ as a function of a single control angle ψ which lies in a plane orthogonal to the spacecraft–Earth vector. This plane $(\hat{\mathbf{e}}_1, \hat{\mathbf{e}}_2)$ is shown in Figure 1.3, where $\hat{\mathbf{e}}_2$ is obtained from the $\hat{\mathbf{e}}_3, \hat{\mathbf{R}}_s$ vectors, with $\hat{\mathbf{e}}_1$ completing the triad. The angle ψ is shown as the angle between $\hat{\mathbf{e}}_1$ and $\hat{\mathbf{u}}$ with $\hat{\mathbf{u}}$ in the $(\hat{\mathbf{e}}_1, \hat{\mathbf{e}}_2)$ plane. The figure also shows the roll, pitch and yaw axes $\hat{\mathbf{e}}_x, \hat{\mathbf{e}}_y, \hat{\mathbf{e}}_z$ at the spacecraft, as well as the solar panels' orientation given by the normal vector $\hat{\mathbf{N}}$ to the panels.

Letting $T_1 = [\hat{\mathbf{e}}_1, \hat{\mathbf{e}}_2]$, the unaveraged state and costate differential equations can be written as

$$\dot{\mathbf{z}} = \frac{2P}{mc}(\mathbf{z}, F, \psi)\, M(\mathbf{z}, F)\, T_1(\mathbf{z}, F) \begin{bmatrix} \cos\psi \\ \sin\psi \end{bmatrix} \tag{1.49}$$

$$\dot{m} = -\frac{2P}{c^2}(\mathbf{z}, F, \psi) \tag{1.50}$$

with $\hat{\mathbf{u}}$ replaced by $T_1(\mathbf{z}, F) = \begin{bmatrix} \cos\psi \\ \sin\psi \end{bmatrix}$ and from